

# Supporting Information

## Structural Correlations of Nitrogenase Active Sites using Nuclear Resonance Vibrational Spectroscopy and QM/MM Calculations

Casey Van Stappen,<sup>1†</sup> Bardi Benediktsson,<sup>2‡</sup> Atanu Rana,<sup>1‡</sup> Aleksandr Chumakov,<sup>3</sup> Yoshitaka Yoda,<sup>4</sup> Dimitrios Bessas,<sup>3</sup> Laure Decamps,<sup>1\*</sup> Ragnar Bjornsson,<sup>1,2,5\*</sup> Serena DeBeer<sup>1\*</sup>

<sup>1</sup>Max-Planck Institute for Chemical Energy Conversion, Stiftstrasse 34-36, 45470 Mülheim an der Ruhr, Germany

<sup>2</sup>Science Institute, University of Iceland, Dunhagi 3, 107 Reykjavik, Iceland

<sup>3</sup>ESRF-The European Synchrotron, CS40220 38043 Grenoble CEDEX 9, France.

<sup>4</sup>Precision Spectroscopy Division, SPring-8/JASRI, Sayo 679-5198, Japan

<sup>5</sup>Univ Grenoble Alpes, CNRS, CEA, IRIG, Laboratoire de Chimie et Biologie des Métaux, 38054, Grenoble, France.

<sup>†</sup>Current Address: Department of Chemistry, University of Texas at Austin, 105 E 24<sup>th</sup> St., Austin, TX 78712

<sup>‡</sup>Current Address: Department of Energy Conversion and Storage, Technical University of Denmark, Anker Engelundsvej 1, Kgs. Lyngby, 2800, Denmark

<sup>‡</sup>These authors contributed equally to this work.

## **Table of Contents**

<b><i>NRVS Data Collection Details.</i></b>	<b>3</b>
<b><i>Figure S1.</i></b>	<b>4</b>
<b><i>Figure S2.</i></b>	<b>4</b>
<b><i>Figure S3.</i></b>	<b>5</b>
<b><i>Figure S4.</i></b>	<b>5</b>
<b><i>Figure S5.</i></b>	<b>6</b>
<b><i>Figure S6.</i></b>	<b>6</b>
<b><i>Figure S7.</i></b>	<b>7</b>
<b><i>Figure S8.</i></b>	<b>7</b>
<b><i>References</i></b>	<b>8</b>

### NRVS Data Collection Details.

Measurements conducted at SPring-8 BL19LXU were performed operating in the C-mode bunch pattern operating at 100 mA with a 145.5 ns interval between X-ray pulses.<sup>1</sup> The incident beam was monochromatized utilizing a high heat load monochromator (HhLM) to obtain an initial ~1 eV bandwidth, followed by a Ge(331)×2Si(975) high resolution monochromator (HRM) to obtain a ~0.8 meV linewidth centred at the nuclear resonance energy (14.4 keV).<sup>2</sup> The monochromatized incident beam flux from BL19LXU was  $5.2 \times 10^9$  photons  $\text{sec}^{-1}$  with a beam size of approximately 0.8 x 1.5 (v x h) mm in FWHM at the time of the measurements. A 5x3 mm<sup>2</sup> silicon-based 2x2 avalanche photodiode (APD) array detector with a 150  $\mu\text{m}$  thick depletion layer<sup>3</sup> was used to detect the delayed <sup>57</sup>Fe nuclear resonance scattering and Fe K fluorescence (from internal conversion) following the nuclear resonance excitation. The strong prompt pulse (from X-ray scattering and fluorescence) was rejected using gating electronics synchronized with the electron bunch clock. An observation time window of 20 to 142 ns after the last bunch in the train was applied. Spectra were collected across an energy range from -30 meV (-241  $\text{cm}^{-1}$ ) to +80 meV (+644  $\text{cm}^{-1}$ ) with respect to the elastic peak position using a step size of ~0.31 meV. A liquid He flow type cryostat was used to provide a low-temperature environment for all measured samples. The Cu block sample holder of the cryostat was held at a temperature of ~15 K for all measurements; however, true sample temperatures ranged from 40-50 K as determined using the S2 detailed balance method available in PHOENIX v.2.1.4.

Measurements conducted at the Nuclear Resonance beamline<sup>4</sup> ID18 of ESRF were performed in the Hybrid 32x12 storage ring operation mode with a nominal ring current of 150 mA. The incident beam was monochromatized with a high heat load 2xSi(111) monochromator (HhLM) to obtain an initial 2.0 eV bandwidth, followed by a 2xSi(4 0 0)+2xSi(12 2 2) high resolution monochromator (HRM) to obtain a 0.63 meV linewidth centred around the nuclear resonance energy (14.4 keV). The monochromatized incident beam flux from ID18 was approximately  $8 \times 10^9$  photons  $\text{sec}^{-1}$  at the time measurements were performed. The beam size on the sample was approximately 0.48 x 0.56 (v x h) mm. An avalanche photodiode (APD) detector with two APD sensors located one immediately after the other was used to detect the delayed <sup>57</sup>Fe nuclear fluorescence following the nuclear resonance excitation. The area and thickness of each sensor was 10×10 mm<sup>2</sup> and 110  $\mu\text{m}$ , respectively. The energy transfer scale was calibrated with a standard  $(\text{NH}_4)_2\text{Mg}^{57}\text{Fe}(\text{CN})_6$  absorber using the narrow three-fold degenerate stretching mode<sup>5</sup> located at room temperature at 74.0(1) meV i.e., at 596.8(8)  $\text{cm}^{-1}$  (as re-evaluated using an IR spectrometer). In order to increase the statistical accuracy of spectra at high phonon energies, data were acquired using “multi-zone” scans, where the energy transfer was scanned with 2 sec/point in the [-10 : 12] meV range, then with 5 sec/point in the [12 : 30] meV range, and finally with 10 sec/point in the [30 : 80] meV range, with 0.25 meV energy grid in all cases. Sample cells were loaded in a liquid He flow cryostat using a Cu block fixed to a cold head maintained at a temperature of ~10 K. True sample temperatures as determined by detailed balance ranged from 30-40 K.

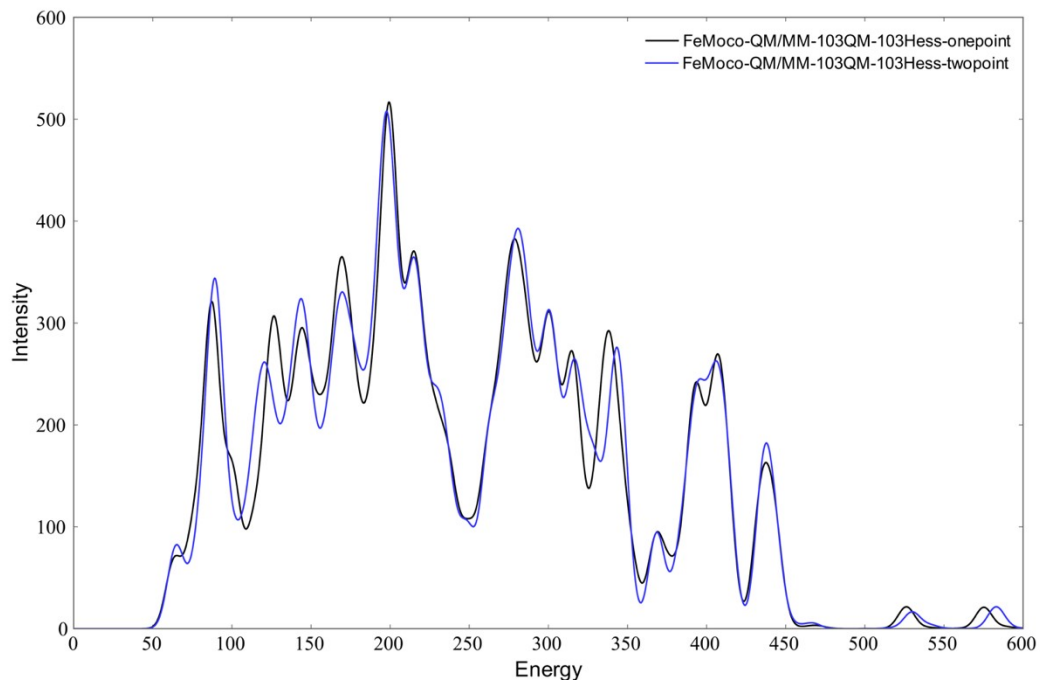


**Figure S1.** Comparison of the QM/MM-calculated numerical Hessian using a 1-point vs. 2-point approximation. QM-region and partial Hessian size is 103 atoms.

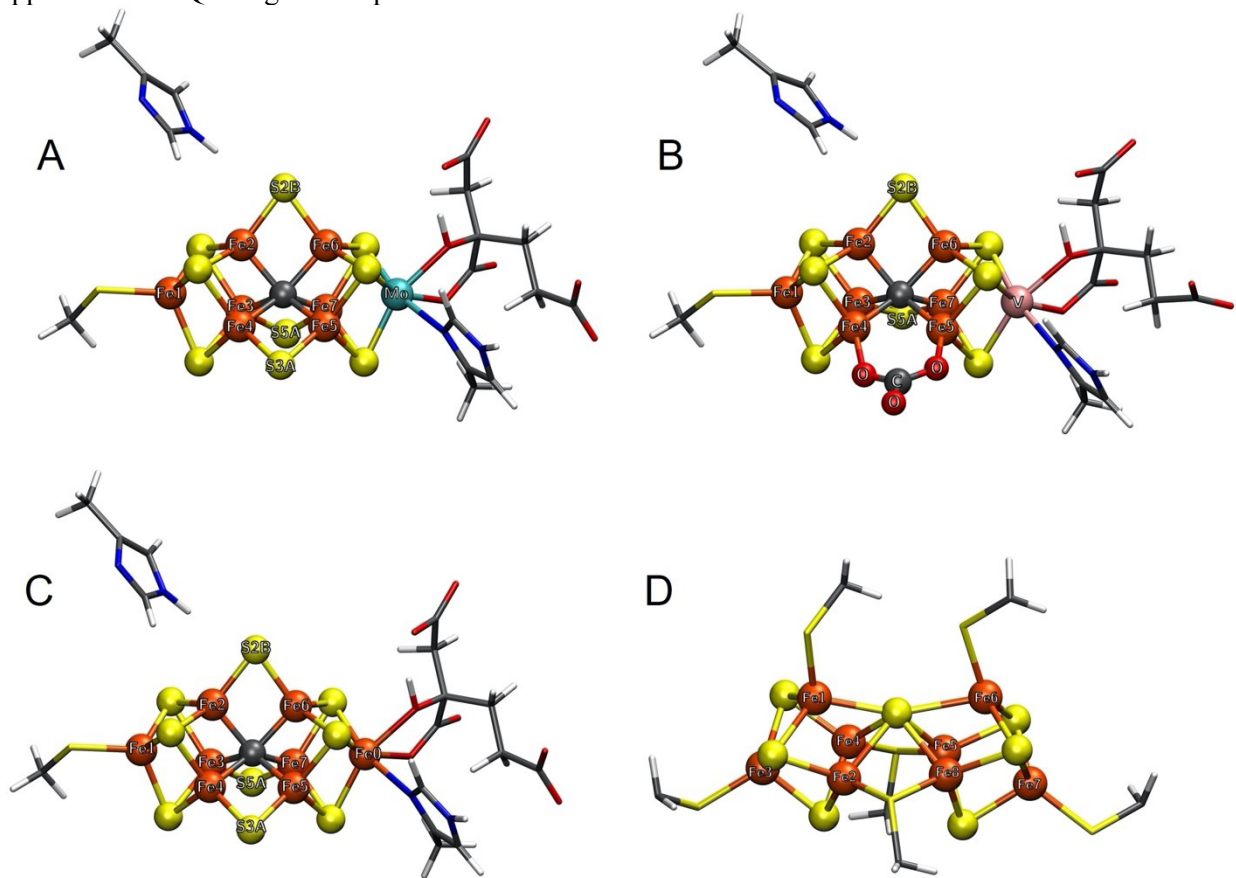


**Figure S2.** Numbering conventions for relative Fe positions of FeMoco, FeVco, FeFeco, and the P-cluster.

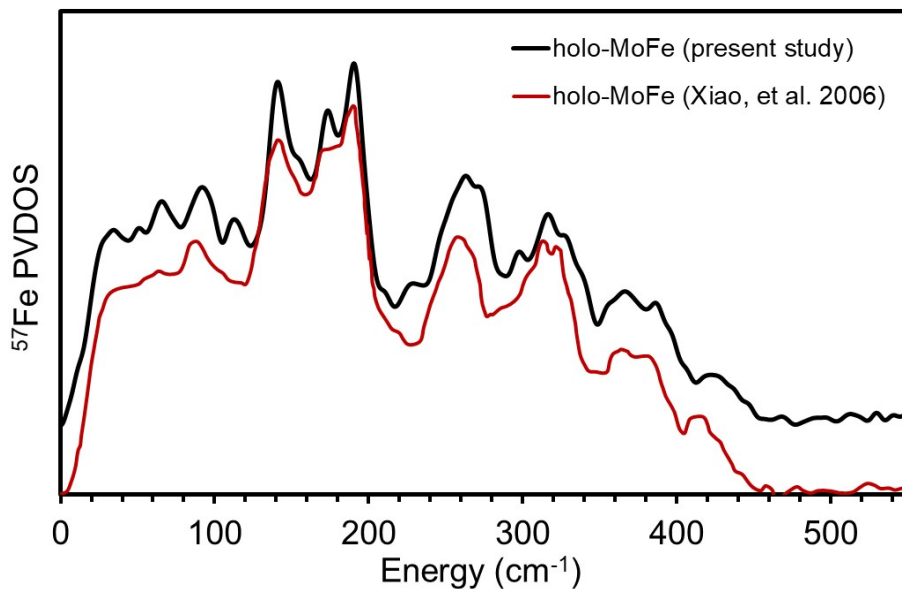


**Figure S3.** A comparison of experimental  $^{57}\text{Fe}$  PVDOS of holo-MoFe protein between our result (black line) vs previously reported (red line).<sup>6, 7</sup> The PVDOS of Xiao, et al. 2006 was adapted with permission from Ref. 1. Copyright 2006 American Chemical Society.

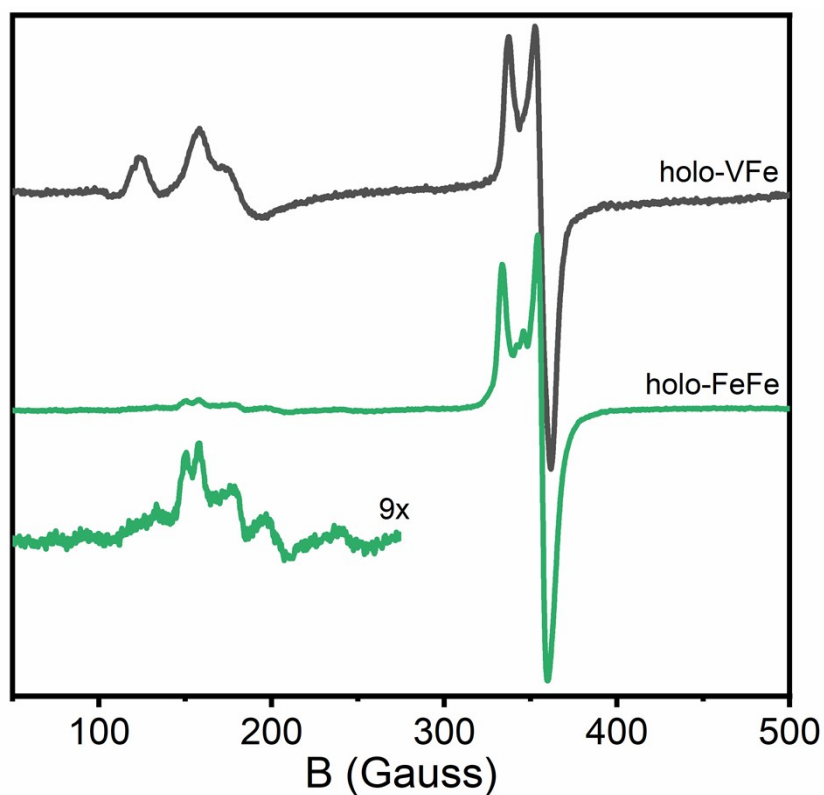


**Figure S4.** CW X-band EPR spectra of holo-VFe (top) and holo-FeFe (bottom) collected for measured NRVS samples.

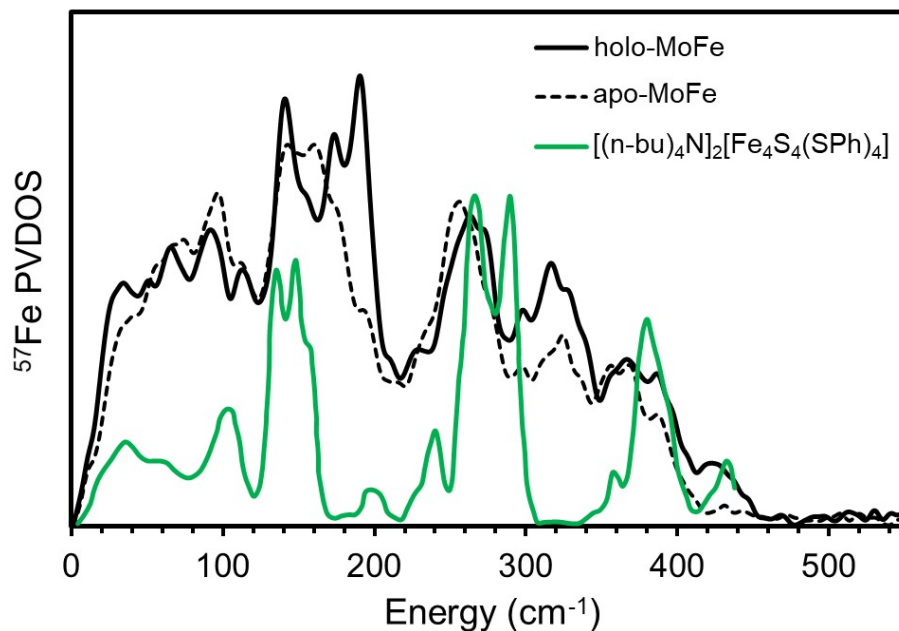


**Figure S5.** An experimental  $^{57}\text{Fe}$  PVDOS overlay of our holo-MoFe (black solid line) and apo-MoFe (black dashed line) protein vs the previously reported PVDOS of  $[(n\text{-Bu})_4\text{N}]_2[\text{Fe}_4\text{S}_4(\text{SPh})_4]$  (green line).<sup>8</sup> The PVDOS of  $[(n\text{-Bu})_4\text{N}]_2[\text{Fe}_4\text{S}_4(\text{SPh})_4]$  was adapted from Ref. 3 with permission from the Royal Society of Chemistry.

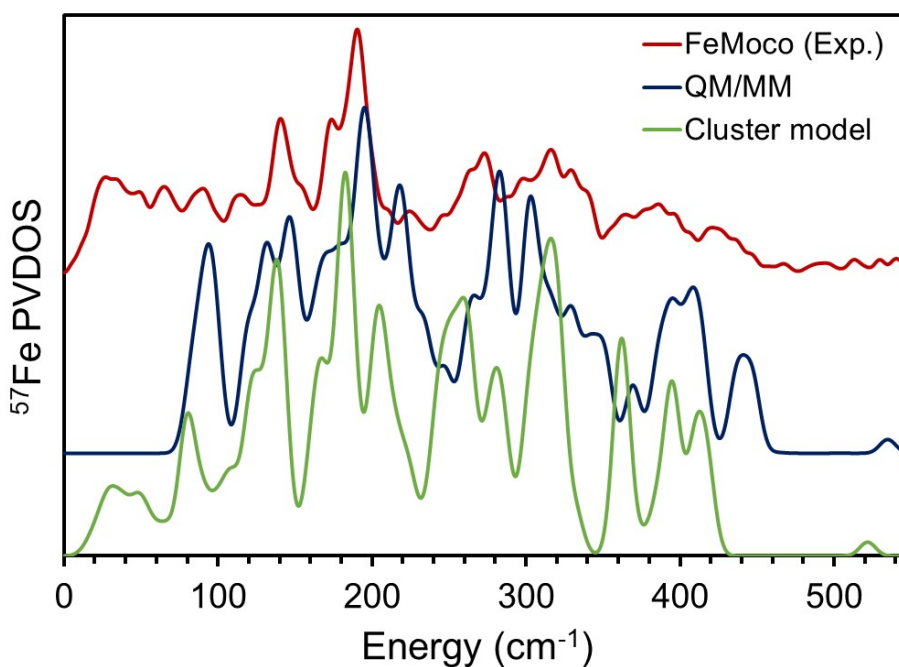


**Figure S6.** An overlay plot of calculated  $^{57}\text{Fe}$  PVDOS of FeMoco using the QM/MM approach with a 54-atom QM-region (blue line) vs. 54-atom CPCM continuum-cluster approach (green line) along with the experimental  $^{57}\text{Fe}$  PVDOS of FeMoco (red line).

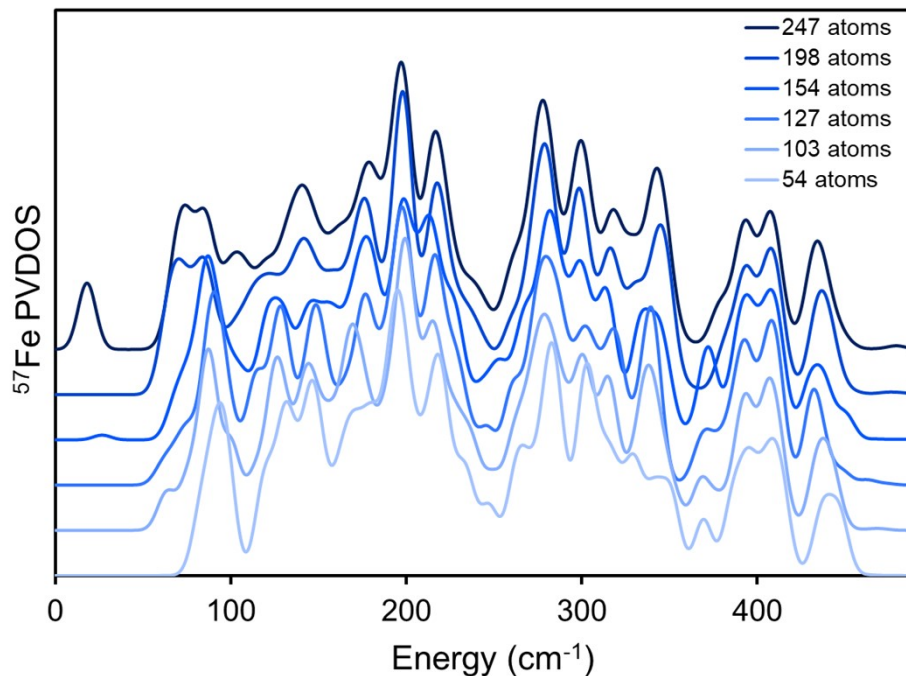


**Figure S7.** An overlay of QM/MM calculated  $^{57}\text{Fe}$  PVDOS of FeMoco with different sizes of the quantum region and partial Hessian. All calculations were performed using the BS7-235 broken-symmetry solution.

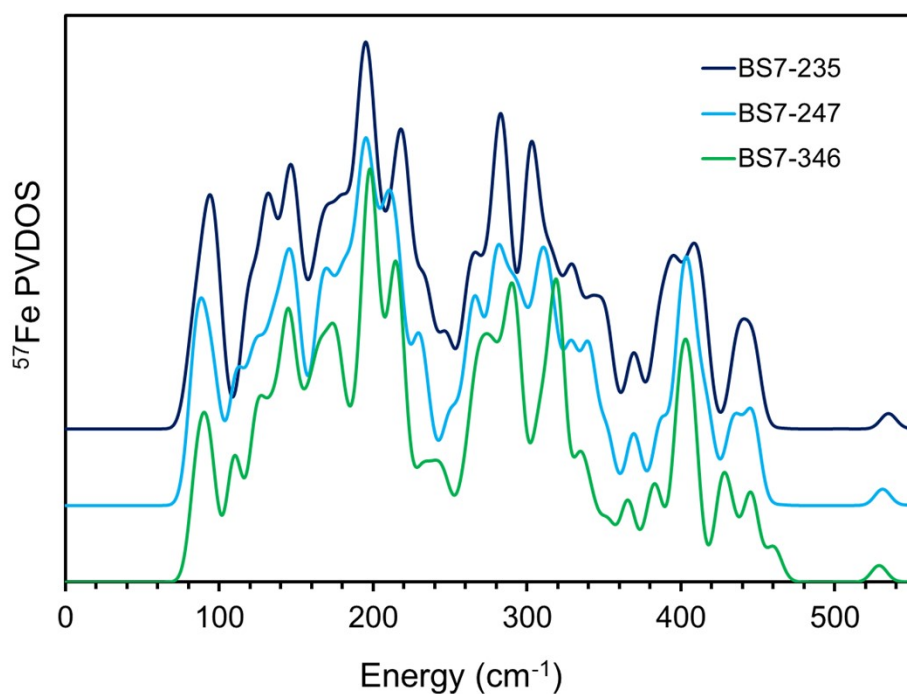


**Figure S8.** A comparison of QM/MM-calculated  $^{57}\text{Fe}$  PVDOS of FeMoco with three different BS7 configurations with  $S = 3/2$  spin state using a 54 atom QM-region and partial Hessian.

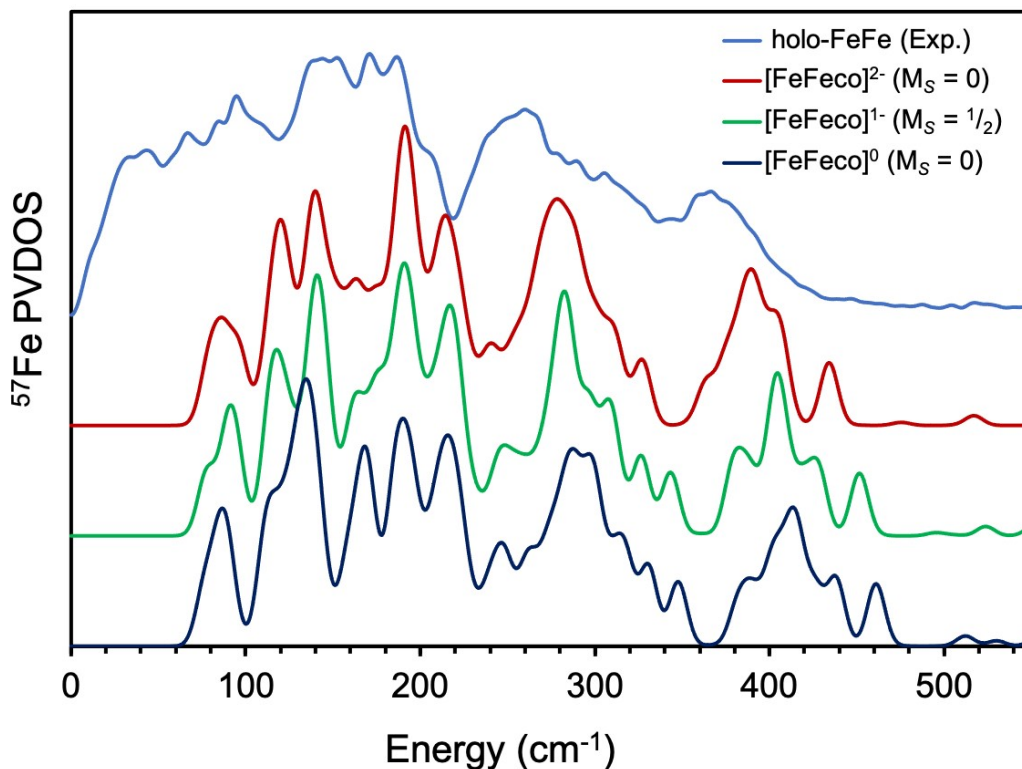


**Figure S9.** A comparison of QM/MM calculated  $^{57}\text{Fe}$  PVDOS of FeFeco in BS7-235 configuration with a combination of different spin states and total charges (as indicated in the figure legend) along with the experimental PVDOS. QM-region and partial Hessian size is 54 atoms.

## References

1. Y. Yoda, M. Yabashi, K. Izumi, X. W. Zhang, S. Kishimoto, S. Kitao, M. Seto, T. Mitsui, T. Harami, Y. Imai and S. Kikuta, *Nucl. Instrum. Methods Phys. Res., Sect. A*, 2001, **467-468**, 715-718.
2. Y. Yoda, K. Okada, H. Wang, S. P. Cramer and M. Seto, *Jpn. J. Appl. Phys. Pt. 1*, 2016, **55**.
3. S. Kishimoto, Y. Yoda, M. Seto, S. Kitao, Y. Kobayashi, R. Haruki and T. Harami, *Nucl. Instrum. Methods Phys. Res., Sect. A*, 2003, **513**, 193-196.
4. R. R uffer and A. I. Chumakov, *Hyperfine Interact.*, 1996, **97**, 589-604.
5. A. I. Chumakov, R. R uffer, O. Leupold and I. Sergueev, *Struct. Chem.* 2003, **14**, 109-119.
6. Y. Xiao, K. Fisher, M. C. Smith, W. E. Newton, D. A. Case, S. J. George, H. Wang, W. Sturhahn, E. Alp, J. Zhao, Y. Yoda and S. P. Cramer, *J. Am. Chem. Soc.*, 2006, **128**, 7608-7612.
7. A. D. Scott, V. Pelenschikov, Y. Guo, L. Yan, H. Wang, S. J. George, C. H. Dapper, W. E. Newton, Y. Yoda, Y. Tanaka and S. P. Cramer, *J. Am. Chem. Soc.*, 2014, **136**, 15942-15954
8. Y. Xiao, M. Koutmos, D. A. Case, D. Coucouvanis, H. Wang and S. P. Cramer, *Dalton Trans.*, 2006, 2192-2201.